

## Eddy-forced coherent structures as a prototype of atmospheric blocking

By KEITH HAINES and JOHN MARSHALL

*Space and Atmospheric Physics Group, Department of Physics, Imperial College, London*

(Received 2 April 1986, revised 10 October 1986)

### SUMMARY

The relevance of nonlinear free solutions of the equivalent barotropic vorticity equation known as ‘modons’ or ‘vortex pairs’ is reconsidered as a prototype of atmospheric blocking. It is argued that modons are highly appropriate reference solutions from which to consider the dynamics of blocks accounting for their local nature, their stability and longevity.

Nonlinear resonance studies with an equivalent barotropic numerical model on a  $\beta$ -plane channel demonstrate the ease and vigour with which vortex pairs can be excited by a vorticity-forcing function of the appropriate form. Localized nonlinear structures which can be identified with modons exist on blocking timescales even in parameter ranges which allow stationary Rossby waves. The circumstances in which synoptic systems can provide an appropriate forcing function are investigated by studying the interaction between a modon and a train of travelling vortices. It is shown that the anomalous transfer of potential vorticity induced by the straining of synoptic systems propagating in a diffluent jet is in a sense to maintain the modon against dissipation. Time sequences of the potential vorticity field from the equivalent barotropic model bear a remarkable resemblance to isentropic potential vorticity maps observed during a blocking episode and suggest that much of the detail can be understood in terms of the passive deformation of baroclinically inactive weather systems.

### 1. INTRODUCTION

The phenomenon of blocking has long been recognized as being of major importance in determining regional climate. Despite having received considerable attention over the past decade it has proved difficult to understand the underlying mechanism of blocking—see Shutts (1983) for a review of blocking theories. It is useful to categorize an approach to the blocking mechanism as either ‘local’ or ‘global’ in character. The global approach considers blocking in terms of planetary Rossby wave resonance in response to orographic/thermal forcing: resonance occurs when almost free Rossby waves are stationary with respect to the ground, the response in a localized region being determined by global-scale forcings. In local theories, on the other hand, emphasis is placed on the local character of blocking from the outset, and we seek to understand blocking as a local nonlinear resonant response to local forcing (see for example McWilliams 1980; Pierrehumbert and Malguzzi 1984, hereafter PM). Such an approach is perhaps more in accord with synoptic observations of blocking and is supported by, for example, the study of Dole and Gordon (1983), who show that blocking events do not appear to be spatially correlated around the globe.

The present study adopts a local approach to blocking and considers the maintenance of local coherent structures against dissipation through their interaction with travelling synoptic-scale systems. It is inspired by the recent potential vorticity diagnostics of planetary-scale flow and blocking presented by Illari (1984), McIntyre and Palmer (1983), Shutts (1986), and for an exhaustive review, see Hoskins *et al.* (1985).

The rapid advance in the quality of routinely produced analysed fields has meant that they can now reveal not only the broad features of the potential vorticity field but also much of the fine detail. For example, the high resolution maps of isentropic potential vorticity (IPV) presented by Shutts (1986) and Hoskins *et al.* (1985) using ECMWF analysed fields, confirm the role of eddies in sustaining blocked configurations. The interaction is revealed at its clearest and most fundamental level in the evolution of the potential vorticity field. The sharp gradient in IPV that marks the partition between high potential vorticity stratospheric air to the north and low potential vorticity tropospheric

air to the south, is seen to undulate north and south as synoptic-scale systems propagate eastwards. On encountering the blocking anomaly the IPV contours are strongly deformed as the synoptic waves steepen and 'break', reversing the meridional potential vorticity gradient and helping to sustain the blocked configuration. These sequences show in a clear and unambiguous way the trajectories of fluid parcels and the irreversible deposition by decaying cyclones of low potential vorticity air on the western flank of the anticyclone. These diagnostic studies of blocking lend a measure of support to the notion that blocking is an essentially local phenomenon in which synoptic-scale systems play a central role in initiation, maintenance and decay. They have encouraged us to consider eddy-forced coherent structures as a prototype of atmospheric blocking. Our study attempts to draw together and extend the investigations of McWilliams (1980), Shutts (1983) and Pierrehumbert and Malguzzi (1984).

McWilliams suggested that many of the observed features of blocking are consistent with nonlinear free mode solutions of the equivalent barotropic vorticity equation which have become known as 'modons' or 'vortex pairs', in which the potential vorticity is constant along streamlines of the flow. Some supporting evidence is provided by potential vorticity diagnostics (see for example Illari (1984) and Shutts (1986)) which indicate that there are often closed height and potential vorticity contours at upper levels. This suggests that modon solutions may be highly relevant in describing the gross features of blocks, accounting for their inherent stability in an otherwise turbulent flow (see also Baines (1983) who likened blocking events over Australia to modons).

PM studied the nonlinear resonance of spatially isolated vortex pairs and, guided by the diagnostic studies of Green (1977) and Illari (1984), speculated that an appropriately signed potential vorticity forcing function could be provided by the eddy flux divergences produced by weather systems propagating around the nonlinear free mode.

Shutts (1983) integrated an equivalent barotropic model to study in more detail the transfer properties of synoptic-scale systems undergoing deformation in a split jet. He showed that the eddy transfer is in a sense to sustain the split jet and, what is more, that it is an inevitable consequence of the eddy-straining mechanism whereby barotropic eddies undergo strong deformation in a diffluent flow and transfer energy up-scale into the straining field.

As a 'zero-order' model of blocking the equivalent barotropic modon is adopted—its analytic construction and relevance to atmospheric blocking is considered in section 2. Section 3 studies the behaviour of synoptic-scale eddies (generated by a wavemaker) impinging upon the modon from the west, simulating conditions at the end of the atmospheric storm tracks. The response of a fully nonlinear equivalent barotropic model to a dipole eddy forcing is then investigated, particular attention being paid to the resonant forcing of the modon considered in section 2. Finally, in section 4, the interaction between finite amplitude synoptic-scale systems and a vortex pair is studied by integrating the fully nonlinear model. Time sequences from this equivalent barotropic model are seen to exhibit a remarkable similarity to the evolution of IPV contours observed during blocking and suggest that much of the detail can be understood in terms of the passive deformation of baroclinically inactive eddies.

## 2. MODONS AS A 'ZERO-ORDER' MODEL OF BLOCKING

Many blocking events consist of a vortex pair embedded in a westerly flow. Figure 1(a) shows the 500 mb height field and Fig. 1(b) the fourth root of the potential vorticity on the 320 K surface during an intense blocking event over N. Europe in February 1983. The synoptic situation is described in Shutts (1986). The thick line in Fig.

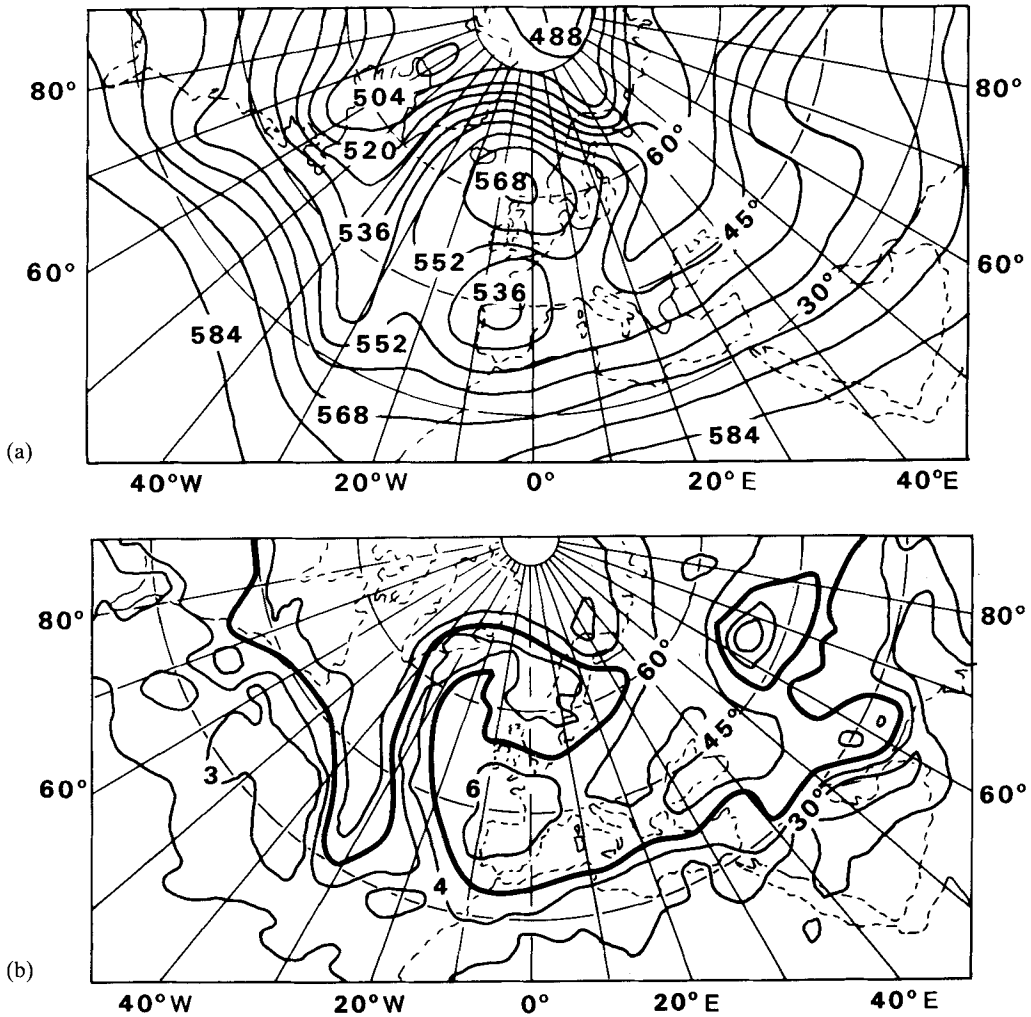


Figure 1. The 500mb height field, (a), contour interval 8 dam; and the fourth root of the Ertel potential vorticity on the 320 K surface, (b), contour interval  $1 \times 10^{-3}$  in m.k.s. units; at 12 GMT on 15 February 1983— from Shutts (1986).

1(b) can be identified with the tropopause which overturns in the vicinity of the block: low potential vorticity air forms the northern portion of the blocking dipole and high potential vorticity air the southern portion. Furthermore, there are closed IPV contours indicating strongly nonlinear behaviour. Winds on the 320 K isentropic surface (not shown) are closely aligned with the IPV contours suggesting that the forcing and dissipation terms are weak and local time-rates of change are small compared with advective timescales. The 'equivalent barotropic modon', a localized solution of the fully nonlinear equivalent barotropic vorticity equation in which the potential vorticity is constant along streamlines of the flow, is plotted in Fig. 2. Evidently there are strong similarities between Figs. 1 and 2 suggesting that such nonlinear free modes may be very useful reference solutions from which to consider the dynamics of blocking configurations and their interaction with synoptic-scale systems. However, an important aspect of the

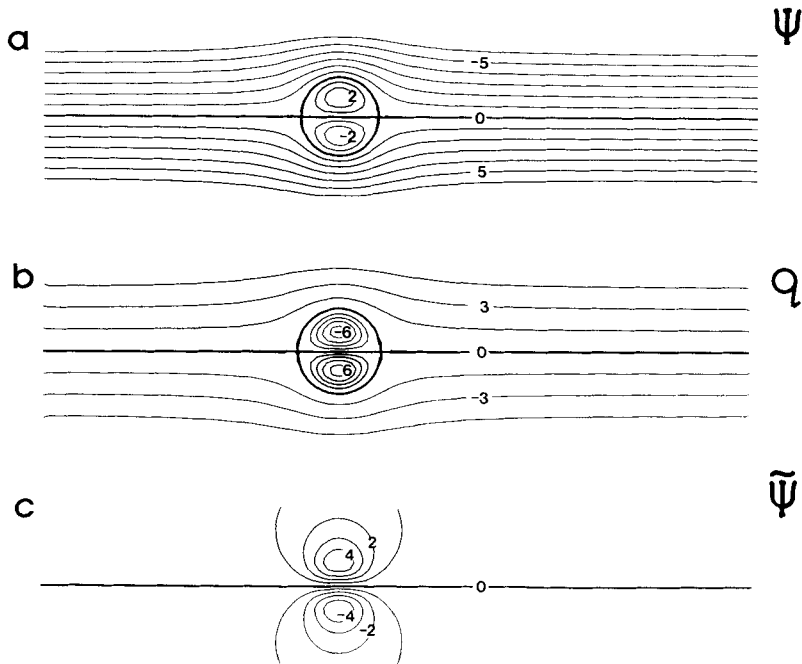


Figure 2. The modon solution Eq. (14) for the parameters Eq. (15). The radius of the modon is 2430 km. The Rossby radius,  $L_p$ , is 845 km,  $\partial q_\infty / \partial y = 1.2\beta$  and  $U = 13.8 \text{ m s}^{-1}$ . (a) Total streamfunction  $\psi$ ; contour interval 1.0. Contours are plotted in units of  $\beta L_p^2$ . A non-dimensional  $\psi$  of unity represents dimensionally a height field perturbation of 9 dam. (b) Potential vorticity  $q$ , contour interval 1.5. Contours are plotted in units of  $\beta L_p$ . (c) The perturbation streamfunction ( $\tilde{\psi} = \psi + Uy$ ). Contours as in (a).  $\tilde{\psi}$  decays to zero at large distances.

dynamics of blocking as revealed by IPV diagnostics, is the large contrast in IPV across the tropopause, which cannot be accommodated within the quasi-geostrophic framework. Without such a contrast it is difficult for advective processes to produce significant upper air IPV anomalies. Quasi-geostrophic theory is a weak anomaly theory and thus is least appropriate near the tropopause where the static stability changes rapidly. Nevertheless despite these reservations we adopt quasi-geostrophy as our dynamical framework since it allows the construction of modon solutions with local closed potential vorticity contours, which we believe to be an important aspect of the blocking mechanism.

The most salient points in the construction of equivalent modon solutions are now reviewed. We begin by emphasizing the role of weak potential vorticity sources and sinks in removing the ambiguities inherent in the inviscid theory.

(a) *Steady-state solutions of the potential vorticity equation*

We consider flows governed by the quasi-geostrophic vorticity equation on a  $\beta$  plane:

$$\partial q / \partial t + J(\psi, q) = \mathcal{F} - \mathcal{D} \quad (1)$$

where  $\psi$  is the streamfunction associated with the geostrophic component of the flow;  $q$  is the quasi-geostrophic potential vorticity

$$q = \nabla^2 \psi + \beta y + f_0^2 \frac{\partial}{\partial z} \left( \frac{1}{N^2} \frac{\partial \psi}{\partial z} \right) \quad (2)$$

$f = f_0 + \beta y$  is the Coriolis parameter with  $f_0$  and  $\beta$  constant

$N^2(z)$  is a reference static stability

$J(a, b) = (\partial a/\partial x)\partial b/\partial y - (\partial a/\partial y)\partial b/\partial x$  is the Jacobian of  $a$  and  $b$

$x$  is east,  $y$  is north,  $z$  is up,  $t$  is time

$\mathcal{F}$  is a potential vorticity source and  $\mathcal{D}$  a potential vorticity sink.

Introducing eddy transfer by separating the flow into a time-mean and eddies, using overbar to represent a time-average long compared with a transient eddy lifetime:  $\psi = \bar{\psi} + \psi'$ ;  $q = \bar{q} + q'$ ; substituting into Eq. (1) and averaging gives

$$\partial \bar{q}/\partial t + J(\bar{\psi}, \bar{q}) = \bar{\mathcal{F}} - \bar{\mathcal{D}} \tag{3}$$

where  $\bar{\mathcal{F}}$  now contains an eddy flux divergence term  $-\nabla \cdot (\bar{\mathbf{v}'q'})$  due to eddy transfer processes which modify the mean flow. Equation (3) can be regarded as describing the evolution of the slowly varying (in time) component of the flow in response to adiabatic and eddy flux divergences associated with the rapidly varying synoptic-scale transients.

We now consider the case of steady ( $\partial/\partial t = 0$ ) almost free ( $\bar{\mathcal{F}} - \bar{\mathcal{D}}$  small) solutions to Eq. (3). Following PM the fundamentally free nature of the circulation can be reflected by writing

$$\bar{\mathcal{F}} - \bar{\mathcal{D}} = \varepsilon \bar{G}$$

where  $\bar{G} = O(|\nabla \bar{\psi}|, |\nabla \bar{q}|)$  and  $\varepsilon$  is a small dimensionless number. The small parameter  $\varepsilon$  has a simple geometrical interpretation as the angle between contours of constant  $\bar{q}$  and contours of constant  $\bar{\psi}$ . This angle is observed to be small at upper levels suggesting that it is useful to expand the fields  $\bar{\psi}$ ,  $\bar{q}$  and  $\bar{G}$ , in terms of  $\varepsilon$ . As shown by PM, Eq. (3) becomes at zero order

$$J(\psi_0, q_0) = 0$$

where  $\psi_0$  and  $q_0$  are the leading-order fields. The general solution can be written

$$q_0 = q_0(\psi_0) \tag{4}$$

i.e.  $q_0$  must be constant along  $\psi_0$  contours. The difficulty with Eq. (4) is that it can allow an infinity of solutions: within any closed contour the functional relationship between  $\psi_0$  and  $q_0$  is quite arbitrary if there is no reference to sources and sinks. However, PM show that not all choices  $q_0(\psi_0)$  can yield a balanced state at  $O(\varepsilon)$  and that a necessary constraint on the zero-order fields is that

$$\int_{\psi_0} \mathcal{F}_0 dx dy = \int_{\psi_0} \mathcal{D}_0 dx dy \tag{5}$$

i.e. potential vorticity sources must balance sinks when integrated over any closed  $\psi_0$  contours. This idea of invoking weak potential vorticity sources and sinks to resolve the ambiguities in the inviscid solution is a development of the Prandtl–Batchelor theorem (Batchelor 1956). It has been extensively used in ocean circulation theory—see for example Niiler (1966), Rhines and Young (1982) and Marshall and Nurser (1986).

The integral balance equation (5) may be particularly important in the study of persistent circulation anomalies such as blocking anticyclones where  $q$  contours are often observed to close off, trapping fluid parcels over local regions. Within these closed  $q$  contour regions, fluid parcels may be exposed to localized forcing leading, through Eq. (5), to a  $q_0(\psi_0)$  relationship which may be different from that outside the blocking region. Indeed it is this change in the functional relationship  $q_0(\psi_0)$  that allows the localized modon solutions with closed  $q$  contours to be analytically constructed.

(b) *Modon solutions*

The standard derivation of modon solutions involves looking for steadily propagating, isolated eddies in a fluid at rest on an infinite  $\beta$  plane; see for example Flierl *et al.* (1980) or McWilliams (1980). In the derivation here however, stationary solutions are derived existing in a uniform zonal flow helping to clarify the relevance of modons to atmospheric blocking.

A solution is sought existing in a zonal flow  $U(z)$ , which is stationary, i.e. of the form Eq. (4),  $q_o = q_o(\psi_o)$ , and isolated. Writing

$$\psi_o = \psi_\infty + \tilde{\psi} \quad (6)$$

where

$$\psi_\infty = -U(z)y$$

is the streamfunction associated with the zonal flow at great distance from the isolated structure and  $\tilde{\psi}$  is the deviation from zonal flow; then for isolation it is required that  $\tilde{\psi}_x = 0$ . Further we define

$$q_o = q_\infty + \tilde{q} \quad (7)$$

where

$$q_\infty = \left\{ \beta - f_o^2 \frac{\partial}{\partial z} \left( \frac{1}{N^2} \frac{\partial U}{\partial z} \right) \right\} \cdot y$$

is the  $q$  field remote from the eddy and

$$\tilde{q} = \nabla^2 \tilde{\psi} + f_o^2 \frac{\partial}{\partial z} \left( \frac{1}{N^2} \frac{\partial \tilde{\psi}}{\partial z} \right) \quad (8)$$

is the deviation of the  $q$  contours from latitude circles associated with the isolated structure.

It is now assumed that the perturbation streamfunction  $\tilde{\psi}$  has 'equivalent barotropic' structure and so can be written in the separable form

$$\tilde{\psi} = A(z)\tilde{\psi}(x, y).$$

Equation (8) then takes the form

$$\tilde{q} = \nabla^2 \tilde{\psi} - \tilde{k}_\rho^2 \tilde{\psi} \quad (9)$$

$$\text{where } \tilde{k}_\rho^2 = -\frac{f_o^2}{A} \frac{\partial}{\partial z} \left( \frac{1}{N^2} \frac{\partial A}{\partial z} \right) = \frac{1}{L_\rho^2}$$

and  $L_\rho$  is an internal Rossby radius of deformation associated with the  $q$  anomaly.

There are difficulties in the interpretation of the equivalent barotropic model in terms of a baroclinic atmosphere. In the present context it may be useful to regard Eq. (9) as a linearized representation of an upper-level potential vorticity anomaly

$$(\zeta + f)/h \approx H^{-1}(\zeta + f - f_o \delta h/H),$$

where  $h = H + \delta h$  is the thickness of an isentropic layer and  $\delta h$  are the perturbations about a mean thickness  $H$ ,  $\zeta$  being the relative vorticity. From this perspective, positive values of  $\tilde{\psi}$  in the blocking high (Fig. 1(a)) are associated with a thickening of isentropic layers, with a raised tropopause and isentropes bowing downward in the troposphere. This is consistent with the observed anomalously low values of static stability just beneath the tropopause in a blocking high; see for example Hoskins *et al.* (1985). Conversely,

negative values of  $\tilde{\psi}$  in the low to the south correspond to a low tropopause, tropospheric isentropes bowing upwards and hence anomalously high values of static stability.

In general Eq. (4) is satisfied if  $q_0$  is constant along  $\psi_0$  contours. In the construction of the modon,  $q_0$  is a different function of  $\psi_0$  inside a circle of radius  $r_0$  where streamlines are closed, than outside this circle where streamlines are open. For analytic convenience linear functional relationships are chosen for both the interior and exterior regions. Thus the equation for  $\tilde{\psi}$  becomes

$$\nabla^2 \tilde{\psi} - \tilde{k}_\rho^2 \tilde{\psi} + (\partial q_\infty / \partial y)y = \alpha(\tilde{\psi} - Uy) \tag{10}$$

where

$$\alpha = \alpha_1 \text{ for } r < r_0, \quad \alpha = \alpha_2 \text{ for } r > r_0.$$

In the far field as  $\tilde{\psi}, \tilde{q} \rightarrow 0$  we require that

$$\alpha_2 = dq_\infty / d\psi_\infty = -(1/U) \partial q_\infty / \partial y \tag{11}$$

which sets the functional relation  $q = \alpha_2 \psi$  for the region  $r > r_0$ . In the near field, still on open contours, we have

$$\nabla^2 \tilde{\psi} = (dq_\infty / d\psi_\infty + \tilde{k}_\rho^2) \tilde{\psi}.$$

For spatially isolated solutions, the exterior field must decay away exponentially (i.e. consist of K Bessel functions in circular-polar coordinates) and so

$$dq_\infty / d\psi_\infty + \tilde{k}_\rho^2 > 0 \quad \text{or} \quad (1/U) \partial q_\infty / \partial y < 1/L_\rho^2 \tag{12}$$

This is precisely the condition that excludes stationary Rossby waves. For  $U > U_m$ , where  $U_m = (1/\tilde{k}_\rho^2) \partial q_\infty / \partial y$ , no stationary Rossby waves are permitted and only spatially isolated structures can be supported. This has important consequences concerning the response of the flow to a localized forcing. For flow speeds  $U > U_m$ , a localized potential vorticity source cannot excite a global response and perturbations will decay away from the source without energy propagation. This is the physics behind the persistence of isolated solutions such as modons for they cannot radiate away energy by exciting stationary Rossby waves in their lee.

It should be noted that in true equivalent barotropic flow for which

$$(1/U) \partial q_\infty / \partial y = \beta/U + \tilde{k}_\rho^2$$

Eq. (12) cannot be satisfied for a westerly airstream since it reduces to  $-\beta/U > 0$ . In order to satisfy Eq. (12) and so prevent Rossby wave radiation, it is necessary that the zonal flow  $U$  advecting the dipole be more barotropic than the dipole itself.

We now turn to the interior solution. On closed streamlines we can see from Eq. (10) that the form of the solution depends on the sign of  $\alpha_1 + \tilde{k}_\rho^2$ . To ensure that the interior solution is finite at  $r = 0$  it must have the form of J or I Bessel functions. If the velocity is required to be continuous at  $r = r_0$  then the interior flow must be wave-like and consist of J Bessel functions, which implies that  $\alpha_1 + \tilde{k}_\rho^2 < 0$  or

$$\alpha_1 < -\tilde{k}_\rho^2. \tag{13}$$

Having chosen  $\alpha_1$  and  $\alpha_2$ , the boundary radius  $r_0$  is determined by matching the velocity,  $\partial \psi / \partial r$ , on the last closed streamline. Thus finally our complete solution can be

written as

$$\left. \begin{aligned}
 \psi &= U \left\{ r_0 \frac{K_1(kr)}{K_1(kr_0)} - r \right\} \sin \theta & \text{for } r > r_0 \\
 \text{where} \quad k^2 &= \tilde{k}_\rho^2 + \alpha_2 \quad \text{and} \quad \alpha_2 = -\frac{1}{U} \frac{\partial q_\infty}{\partial y} \\
 \text{and} \\
 \psi &= U \frac{k^2}{k'^2} \left\{ r - r_0 \frac{J_1(kr)}{J_1(kr_0)} \right\} \sin \theta & \text{for } r < r_0 \\
 \text{where} \quad k'^2 &= -(\tilde{k}_\rho^2 + \alpha_1).
 \end{aligned} \right\} \quad (14)$$

It should be noted that the relationship between  $\psi$  and  $q$  is not analytic over the whole plane; indeed the solution is localized because  $dq/d\psi$  changes discontinuously at  $r = r_0$  becoming more negative on closed  $q$  contours. The double-valued functional relationship  $q(\psi)$  is chosen for analytic convenience allowing the construction of exact finite amplitude solutions. However, in section 2(a) it was shown that  $q(\psi)$  within closed contours may be set by source/sink balances according to Eq. (5) and so it is not unreasonable to expect rather rapid changes in  $q(\psi)$  on moving from open to closed  $q$  contours. In contrast, Malguzzi and Malanotte-Rizzoli (1984) construct weakly nonlinear dipole solutions that are trapped in a mean flow with a continuously varying relation  $q(\psi)$ . The mean flow, however, is entirely zonal and the perturbations are weak so the changes in  $q(\psi)$  are not associated with the closing off of  $q$  contours.

### (c) Mean flow parameters

McWilliams (1980) has made a detailed comparison between a winter Atlantic blocking episode and analytic solutions of the form Eq. (14). He found that for the vertically and zonally averaged tropospheric state the existence condition, Eq. (12), is not easily satisfied. However, this may not be surprising since isolated structures are not observed to persist at all longitudes and levels. McWilliams points out that if blocking were indeed a local phenomenon then the zonal, height- and time-averaged state may not be the most appropriate with which to test the analytic theory. A definitive observational study has yet to be made. However, it should be noted that Eq. (12) is most easily satisfied in regions of strong flow and weak potential vorticity gradients (as might be found at upper levels at the end of the storm track) and large  $\tilde{k}_\rho$  (shallow layers of low static stability); these are precisely the conditions pertaining during Atlantic blocking episodes.

From the analysis given in section 2(b) there are four parameters which must be defined to construct an equivalent barotropic modon;

two associated with the zonal flow:

$$\begin{aligned}
 U & - \text{uniform zonal flow speed} \\
 \partial q_\infty / \partial y & - \text{ambient potential vorticity gradient}
 \end{aligned}$$

and two with the isolated structure:

$$\begin{aligned}
 \tilde{k}_\rho^2 &= 1/L_\rho^2 \text{ where } L_\rho \text{ is a deformation radius} \\
 \alpha_1 &= dq/d\psi \text{ within the closed } q \text{ contour region.}
 \end{aligned}$$

The values given below define the analytical modon solution shown in Fig. 2, and were used to initialize our numerical experiments, except where otherwise stated.



$$\left. \begin{aligned} U = 13.8 \text{ m s}^{-1}; \quad \partial q_{\infty} / \partial y = 1.2\beta; \quad \beta = 1.6 \times 10^{-11} \text{ m}^{-1} \text{ s}^{-1}; \\ L_{\rho} = 845 \text{ km}; \quad \alpha_1 = -3.9 \times 10^{-12} \text{ m}^{-2}. \end{aligned} \right\} \quad (15)$$

These parameters, which just satisfy the condition Eq. (12), give a modon with a radius  $r_0 = 2430 \text{ km}$  and a maximum velocity at the edge of  $28.9 \text{ m s}^{-1}$ .

Illari and Marshall (1983) have plotted  $\bar{q}$  (quasi-geostrophic) against  $\bar{\psi}$  on the 300 mb surface over a block and from their Fig. 7a we deduce a mean  $d\bar{q}/d\bar{\psi}$  of  $-4 \times 10^{-12} \text{ m}^{-2}$ . This value is close to  $\alpha_1$  chosen for the interior of the analytic modon defined above, although the measured value is more appropriate to open contour regions (see Illari and Marshall, Fig. 6a, which shows the corresponding  $\bar{q}$  field).

### 3. EDDY FORCING OF LOCALIZED STRUCTURES

Numerical integrations of the equivalent barotropic vorticity equation in a  $\beta$ -plane channel initialized with the analytic solution Eq. (14) attest to the remarkable stability of this structure: although it is a solution existing on an infinite  $\beta$  plane and  $\partial q / \partial r$  is discontinuous at  $r = r_0$ , it remains stable in the numerical model with very little boundary adjustment. But suppose now a weak dissipative process is introduced through a surface Ekman layer  $\mathcal{D} = \mathcal{E} \nabla^2 \psi$  or a Newtonian damping term proportional to  $\tilde{\psi}$ , then in order that in an integral sense the localized structure be maintained against dissipative processes, a forcing term of the appropriate sign must be present to satisfy the condition Eq. (5). Since the modon solution Eq. (14) has a north-south vorticity dipole, a north-south structure in the forcing  $\mathcal{F}$  is required to offset the dissipation  $\mathcal{D}$ , with anticyclonic forcing to the north and cyclonic forcing to the south. There is now much theoretical and observational evidence that this dipole vorticity forcing can be provided by, and moreover is an inevitable consequence of, the anomalous transfer of vorticity by synoptic-scale systems propagating in a diffluent jet upstream of a blocking dipole. Shutts (1983) and Illari and Marshall (1983) have argued that the split jet acting as a deformation field on the synoptic systems, organizes them in such a way that the split can be sustained by them: the north/south dipole eddy vorticity forcing found in the diagnostic study of Illari (1984) is a natural consequence of the transfer properties of synoptic-scale systems which undergo a compression of their east/west scale as they move into a region of weak zonal flow. Shutts (1986) and Hoskins *et al.* (1985) discuss this interaction in terms of IPV and remind us how perceptive were the early synoptic studies presented by, for example, Berggren, Bolin and Rossby (1949). In this section the interaction of isolated modon solutions with synoptic-scale systems is investigated to gain further insight into the above mechanism.

The action of large-scale eddies will be imagined to occur schematically in the following three stages.

First, the genesis of eddy vortices (cyclonic and anticyclonic) by baroclinic processes; second, the quasi-barotropic redistribution of eddy activity (bowing of trough lines due to the  $\beta$  effect and differential advection due to the curvature of the wind); and third, the consequent feedback of the eddies on the mean flow. Of course this is somewhat of an idealization, but it is considered to be a useful one.

In our model the first of these phases is parametrized by a wavemaker which can be interpreted as representing vortex stretching,  $f \partial w / \partial z$ , associated with baroclinic processes. The second phase is modelled by explicit integration of the equivalent barotropic vorticity equation linearized about a free solution  $q_0 = q_0(\psi_0)$ , in this case the modon of Eq. (14):

$$\left. \begin{aligned} \partial q' / \partial t + J(\psi_0, q') + J(\psi', q_0) &= \mathcal{F}' - \mathcal{D}' \\ q' &= \nabla^2 \psi' - \tilde{\kappa}_\rho^2 \psi' \end{aligned} \right\} \quad (16)$$

where  $q'$ ,  $\psi'$  are transient eddy components. Equation (16) is forced by a wavemaker  $\mathcal{F}'$  which successively introduces vorticity of opposite signs in a localized region upstream of the modon. This eddy activity is advected and dispersed downstream permitting a study of the passive deformation of synoptic-scale systems by the split jet. The correlations of  $\mathbf{v}'$  and  $q'$  are computed and the eddy flux divergence term evaluated.

The third phase, that is the effect of the eddies on the mean flow, is investigated by integration of the mean flow equation

$$\partial \bar{q} / \partial t + J(\bar{\psi}, \bar{q}) = -\nabla \cdot (\bar{\mathbf{v}}' \bar{q}') - \bar{\mathcal{D}} \quad (17)$$

where

$$\bar{\psi} = -Uy + \tilde{\psi}; \quad \bar{q} = (\partial q_\infty / \partial y)y + \tilde{q}; \quad \tilde{q} = \nabla^2 \tilde{\psi} - \tilde{\kappa}_\rho^2 \tilde{\psi}$$

to a steady state where rectification of the eddy fields computed in Eq. (16) now appears as a forcing term in Eq. (17).

A  $\beta$ -plane second-order finite difference numerical model is used to integrate Eqs. (16) and (17). The Arakawa (1966) scheme is used to evaluate the Jacobian terms at interior and boundary points, and a leap-frog scheme employed to step forward in time. At each time-step a finite difference form of the elliptic equation is inverted exactly to solve for  $\psi$  from  $q$ .

The form of  $\mathcal{F}'$  is described in Shutts (1983) section 4(c), and ensures that  $\overline{\mathcal{F}'}^{xy} = 0$  for all time. Thus the wavemaker cannot itself directly drive mean flows (it does not appear in Eq. (17)). It is judiciously chosen so as to successively introduce vortices of alternating sign well upstream of the modon. A scale-selective grid-point diffusion term  $\nu \nabla^6 \psi'$  is adopted for  $\mathcal{D}'$  which efficiently destroys enstrophy at the grid-scale of the model. The coefficient  $\nu$  is reduced to the minimum required to maintain a smooth potential vorticity field. In addition to the specification of the streamfunction at the channel walls (determined by invoking a zonal momentum constraint to give the pressure drop across the channel) the  $\nu \nabla^6 \psi'$  term requires two additional boundary conditions: the 1st and 3rd derivatives of the vorticity normal to the wall are set to zero ensuring that this term cannot act as a net vorticity sink.

Equation (16) is solved in a rectangular domain of repeat distance 44 800 km and width 10 500 km on a square finite difference grid at 350 km resolution. A large channel width is chosen so as to ensure that the walls do not interfere with the evolution of the modon, which we recall is a solution of the steady inviscid equations on an infinite  $\beta$  plane. The channel is chosen to be sufficiently long to allow the modon to be isolated from the region of eddy production and to ensure that eddy energy does not recycle.

#### (a) Eddy forcing pattern

Consider first introducing eddy vortices into a linearized model with uniform zonal flow  $U$  and ambient potential vorticity gradient  $\partial q_\infty / \partial y$ . If account is taken of the variation in  $f$  with latitude then the axes of the eddy streamlines must become bow-shaped, because the induced motions outside the genesis region correspond to Rossby waves which travel rather rapidly to the west leading to a characteristic bowing of trough lines. On consideration of the attendant Reynolds stresses the vorticity transfer is easily deduced, being northwards at the latitude of the genesis region and southward to the north and south. This leads to cyclonic forcing to the north, anticyclonic forcing to the south, tending to accelerate the flow eastward at the jet axis and decelerate it elsewhere. But

what happens if the eddy vortices are advected into a region of diffuence such as a blocking anticyclone? To investigate, Eq. (16) is integrated forward from  $\psi'$  and  $q' = 0$  at time 0 by introducing vorticity from a wavemaker  $\mathcal{F}'$  placed in the zonal flow far upstream of the modon given by Eqs. (14) and (15). An Ekman dissipation term  $\mathcal{D}' = \mathcal{E}\nabla^2\psi'$  was included with a spin-down timescale  $\mathcal{E}^{-1} = 10$  days.

Figure 3 shows the eddy flux divergence pattern  $\nabla \cdot (\bar{\mathbf{v}}'q')$ . The important feature to note is the marked north/south, divergence/convergence dipole upstream of the modon in the split jet which is in the opposite sense to that deduced above. This pattern of eddy forcing is understandable in rather general terms (see, for example, Shutts (1983); Illari and Marshall (1983)). The split jet acts as a strong deformation field on the waves impinging on it. A study of a sequence of instantaneous fields shows that the eddies suffer an east/west compression and meridional extension as they are advected up toward the modon and are subsequently strongly deformed by the split jet. Associated with this strong deformation, there is a transfer of energy up-scale into the straining field (the  $\psi_0$  flow) and a concomitant down-scale transfer of enstrophy, with potential vorticity fluxes directed systematically down-gradient, to be balanced by the dissipation of enstrophy at the grid-scale of the model. The divergence of this down-gradient southward flux gives the reverse dipole in the eddy forcing pattern centred on the split jet evident in Fig. 3.

This general reverse dipole pattern of eddy forcing at the end of the storm track is insensitive to the detailed form chosen for  $\psi_0$  provided it has a diffluent structure. This is borne out by the numerical experiments of Shutts (1983) and observational studies of Illari (1984) and Shutts (1986). Shutts chose a stationary Rossby wave with dipole meridional structure for  $\psi_0$  and obtained a broadly similar eddy forcing pattern. Illari found a dipole eddy forcing at 300 mb centred on the split jet in a diagnostic study of atmospheric blocking using analysed fields. Such a forcing pattern is also implicit in the 'E-vector' diagnostics presented in Hoskins *et al.* (1983).

Before going on to consider the induced flow we note that the eddy potential vorticity forcing pattern at the end of the storm track in Fig. 3 has precisely the form required to satisfy Eq. (5) and hence maintain the anomalous potential vorticity field, against dissipation: anticyclonic to the north and cyclonic to the south. We now study the resonant forcing of dipole structures by using the forcing  $\mathcal{F}$  obtained from the linearized model as a time-independent vorticity source in Eq. (17). In these experiments the eddy forcing pattern downstream of the vertical line in Fig. 3, associated with the interaction of eddies

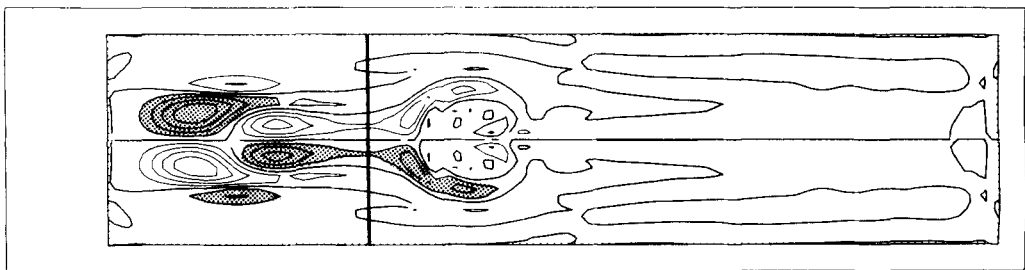


Figure 3. Eddy flux divergence  $\nabla \cdot (\bar{\mathbf{v}}'q')$  computed by averaging a 25-day sequence of synoptic maps from the model, Eq. (16), linearized about the modon solution, Eqs. (14) and (15). The channel is 44 800 km long and 10 500 km wide. Regions of convergence are shaded: the pattern is antisymmetric about mid-channel. The convergence to the north of the storm track and divergence to the south coincide with the wavemaker. The reverse dipole (divergence to the north, convergence to the south) at the end of the storm track (downstream of the vertical line) is induced by the straining of eddies in the split jet upstream of the modon. This reverse dipole is in the correct sense to maintain the modon against dissipation.

with the modon, was used as a potential vorticity source in Eq. (17). This dipole forcing was positioned near the re-entrance region at the upstream end of the channel.

(b) *Induced mean flow*

We expect to see evidence of two distinctly different responses depending on whether fluid parcels can be trapped over the forcing region (i.e. whether locally there are open or closed  $q$  contours).

If Eq. (12) is satisfied, disallowing global Rossby modes, then we expect a local response to local forcing. If the  $q$  contours close off over the forcing region, fluid parcels become trapped and resonance is possible with an appropriately signed vorticity source. As discussed in PM this can appropriately be called a nonlinear local resonance. It is closely related to, but distinctly different from the familiar linear resonance, in which stationary Rossby waves are the inviscid solutions. In this case the  $q$  contours are open and the response is global. Fluid parcels are not trapped but sample forcing/dissipation over the whole channel. In the conventional linearized model (about a zonal flow  $U$  in a  $\beta$ -plane channel for example) the resonant points form a discrete set determined by model geometry and the basic state flow field. In nonlinear systems the resonant points are not so dependent on model geometry such as the width and repeat length of the channel.

It is not yet clear to what extent the atmosphere reflects these different responses but they can be conveniently demonstrated and studied in our numerical model. Thus Eq. (17) is integrated using the eddy flux divergence pattern  $\nabla \cdot (\mathbf{v}'q')$  (over the modon region shown in Fig. 3) as a time-independent forcing. The magnitude of the forcing is scaled up from the linearized model to give a maximum forcing of  $3.3 \times 10^{-10} \text{ s}^{-2}$ , consistent with the eddy  $q$  flux divergences found by Illari (1984) at 300 mb in a blocking episode. Dissipative processes are represented through an Ekman layer,  $\mathcal{E} \nabla^2 \psi$ , again with a spin-down time of  $\mathcal{E}^{-1} = 10$  days.

(i) *'Modon' response.* The mean flow  $U$  and  $\partial q_\infty / \partial y$  are chosen to satisfy condition Eq. (12) (see legend of Fig. 4 for details); there are no stationary Rossby modes allowed in the channel and so global resonances are not possible. Instead a local nonlinear free mode is resonantly excited in the region of the forcing. A structure resembling the analytic solution of Fig. 2 grows up with many closed  $q$  contours trapping fluid over the forcing—see Fig. 4. The intensity of the circulation is limited by bottom friction. However, the isolated dipole is not completely steady: an exact integral balance between forcing and dissipation is not wholly achieved, leading to some residual time evolution. The

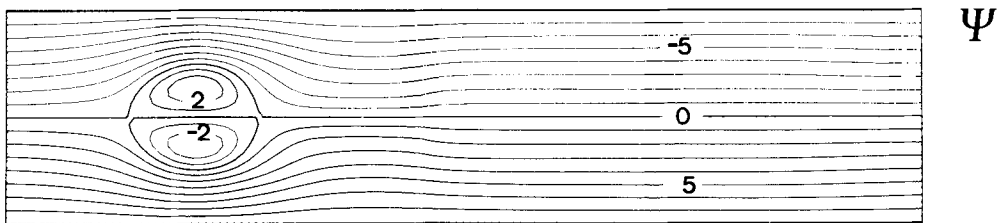


Figure 4. The resonant streamfunction ( $\psi$ ) response after 50 days, obtained by integrating the fully nonlinear model Eq. (17) forced by a dipole potential vorticity source. The eddy flux divergence pattern downstream of the vertical line in Fig. 3 is used as the forcing function. It has a maximum amplitude of  $3.3 \times 10^{-10} \text{ s}^{-2}$ . An Ekman dissipation term is present with  $\mathcal{E}^{-1} = 10$  days. The zonal velocity  $U = 13.8 \text{ m s}^{-1}$  and potential vorticity gradient  $\partial q_\infty / \partial y = 1.12\beta$  are chosen to exclude stationary Rossby waves i.e.  $dq_\infty / d\psi_\infty + k_p^2 > 0$ . The vortex pair amplifies rapidly, spectacularly demonstrating a nonlinear resonance. Contours are plotted in units of  $\beta L_p^3$  as in Fig. 2.

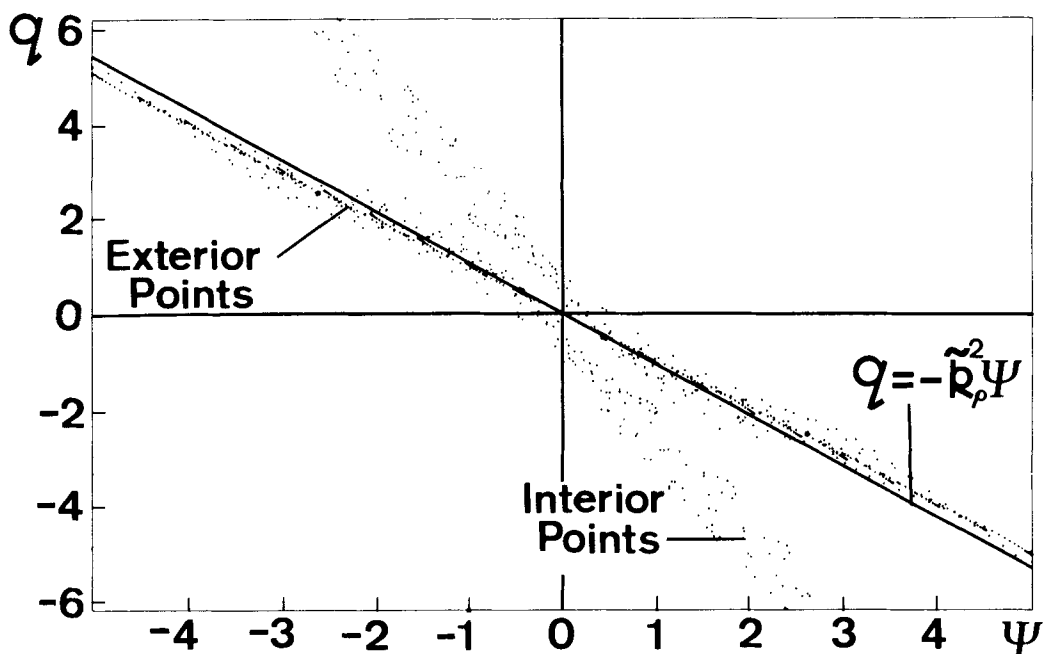


Figure 5. The  $q/\psi$  scatter diagram for the instantaneous field of Fig. 4 showing distinctive ‘modon’ characteristics. The points fall onto two distinct straight lines, the steeper corresponding to points on closed streamlines, the gentler corresponding to those on open streamlines. Between them lies the continuous line of slope  $-\tilde{k}_\rho^2$ ; evidently the modon existence condition, Eq. (12), is satisfied.  $\psi, q$  are in units of  $\beta L_\rho^3, \beta L_\rho$ , respectively.

vortex pair drifts across the forcing region, its intensity fluctuating markedly depending on its position relative to the forcing. When it is seated squarely over the dipole forcing it amplifies rapidly, spectacularly demonstrating a local nonlinear resonance.

The  $q/\psi$  scatter plot in Fig. 5 shows that there is a good functional relationship between  $q$  and  $\psi$  indicating that forcing and dissipation are not  $O(1)$  terms locally in the vorticity equation: the solution is still almost a free mode. The plot shows two different linear functions, one for points on closed  $q$  contours and one for points on open  $q$  contours. These slopes are consistent with those of the analytic modon, with  $dq/d\psi$  being more negative on closed  $q$  contours than open ones. It is worth remarking on the linearity of the functional relationships particularly interior to the modon; presumably there are nonlinear functional relationships between  $q$  and  $\psi$  which equally well satisfy the unforced, undamped equations, but the resonantly excited response chooses a linear  $q(\psi)$  relation. The small scatter of points about the straight line indicates adjustment to source/sink terms as described in section 2. Also plotted in Fig. 5 is a line with slope  $-\tilde{k}_\rho^2$  near which most of the exterior points congregate. It can be seen that the mean flow condition, Eq. (12), is just satisfied:  $\tilde{k}_\rho^2$  is large enough to exclude the possibility of exciting wavy solutions in the far-field.

The dipole forcing has thus resonantly excited a response which can be identified with the free mode solution, Eq. (14). However, it is the integral balance between (weak) forcing and dissipation which helps to fix the amplitude and scale of the solution (in inviscid theory the amplitude and scale are arbitrary). This is now considered in more detail.

Assuming a steady state, the integral balance, Eq. (5), becomes, integrating over

the area enclosed by the outermost closed streamline of the modon,

$$C = (1/\varepsilon) \int_{\psi} \overline{\mathcal{F}} dx dy \quad (18)$$

where  $C = \oint \mathbf{v} \cdot d\mathbf{l}$  is the circulation and  $\int \overline{\mathcal{F}} dx dy$  is the net vorticity forcing over, say, the northern anticyclonic vortex of the modon shown in Fig. 4.

From Eq. (14) the circulation  $C$  can be evaluated analytically. It can be shown that for a wide spectrum of modon size and intensity, the circulation is given to a good approximation by

$$C = \gamma U_0 r_0 \quad (19)$$

where  $U_0$  is the maximum velocity at the edge of the modon (corresponding to  $\theta = \pi/2$ ), and  $\gamma$  is a constant. Furthermore for modons of a size and intensity of meteorological interest,  $\gamma$  is a constant close to  $\pi$ ; Eq. (19) thus gives a relation between  $U_0$  and  $r_0$ .

From the exterior solution (differentiating Eq. (14))

$$U_0 = U k r_0 K_2(kr_0)/K_1(kr_0) \quad (20)$$

giving another relation between  $U_0$  and  $r_0$  since  $U$  and  $k$  are known. Thus Eqs. (19) and (20) can be solved for  $U_0$  and  $r_0$  given the circulation  $C$  in terms of forcing and dissipation balances, Eq. (18). Explicitly the dependence of the modon radius  $r_0$  on forcing and dissipation is given by

$$X^2 K_2(X)/K_1(X) = kC/\gamma U \quad \text{where } X = kr_0 \quad (21)$$

and  $C$  is set by Eq. (18).

For the magnitude of the forcing and dissipation chosen in Fig. 4,

$$(1/\varepsilon) \int \overline{\mathcal{F}} dx dy = -3.47 \times 10^8 \text{m}^2 \text{s}^{-1}$$

(integrating over the northern half of the dipole) and the mean flow parameters given in the figure legend, solving Eq. (21) gives, for  $\gamma = \pi$ , a radius  $r_0$  of 3050 km. This compares favourably with the radius of the outermost closed  $q$  contour observed in Fig. 4 of 2600 km.

The major source of error committed in deriving Eq. (21) is the assumption of a steady state leading to Eq. (18). The modon shown in Fig. 4 is, in fact, evolving and so at any instant there is not an exact balance between forcing and dissipation, the residual resulting in time dependence  $dC/dt$ .

Nonlinear resonances of the type described here have been studied in the context of the blocking mechanism by PM. They adopted an analytic expression for the forcing, to exactly balance an Ekman dissipative term. Here it has been explicitly demonstrated that a forcing of the appropriate form can be effected by anomalous eddy transfer by synoptic-scale systems and, further, that the nonlinear free mode that such a forcing excites is very close to the equivalent barotropic modon of McWilliams (1980). It is important to realize that Eq. (5) is an integral statement and so the form of the response is not sensitive to the details of the forcing: it is only necessary that it has an appropriate dipole form.

(ii) *Stationary Rossby wave response.* When Eq. (12) is not satisfied, for example at slower flow speeds or stronger potential vorticity gradients, it is possible to excite global modes of the channel. Figure 6 shows a familiar damped Rossby wave response resonantly excited by the eddy forcing pattern, now in a model linearized about the same zonal flow

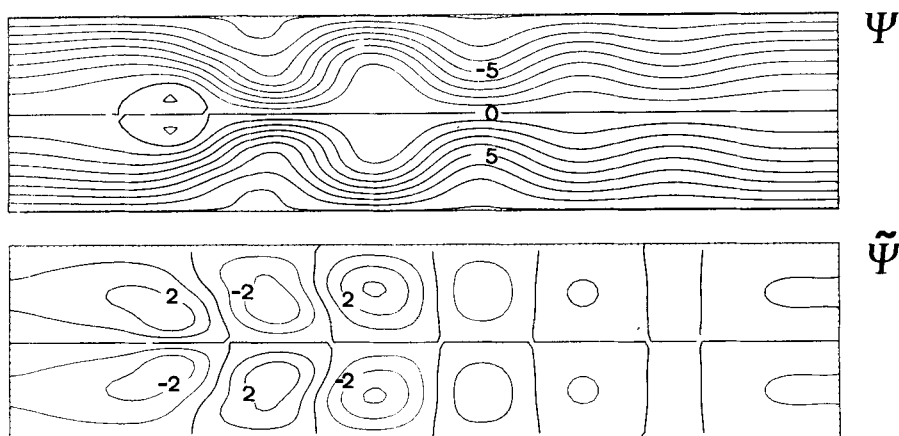


Figure 6. The steady state streamfunction field after 75 days of integration with the model Eq. (17) linearized about a zonal flow  $U = 13.8 \text{ m s}^{-1}$ ,  $\partial q_\infty / \partial y = 1.81\beta$ . Stationary Rossby waves are allowed in the channel with  $dq_\infty/d\psi_\infty + \bar{k}_p^2 < 0$ . The forcing and dissipation are the same as in Fig. 4. An antisymmetric Rossby wave is excited in the lee of the vorticity forcing dipole. Contours are plotted in units of  $\beta L_p^2$ .

model is linearized about a zonal flow there is no possibility of trapping fluid parcels over the forcing region as in the nonlinear resonance of Fig. 4. Instead, on each circuit of the channel, fluid parcels receive an impulse of potential vorticity at the dipole source setting up a Rossby wave train which slowly decays away as the fluid parcels lose their vorticity through weak bottom friction. By the time the fluid parcels have completed a circuit of the channel they have dissipated the vorticity imparted to them. The zonal decay scale depends on the magnitude of the bottom friction coefficient. Essentially this is the mean flow response obtained by Shutts (1983) who resonantly excited an antisymmetric stationary Rossby wave with a dipole eddy forcing produced downstream of a wavemaker—see, for example, Fig. 6(a) of Shutts (1983).

The response of this flow (Eq. (12) not satisfied) to the dipole forcing but with the nonlinear terms retained, exhibits characteristics of both Figs. 4 and 6, i.e. local and global responses. In the early stages of the integration (see Fig. 7(a)) there is a resonant response local to the forcing which has distinctive ‘modon’ characteristics. Fluid parcels are trapped over the forcing region allowing rapid amplification. Indeed, scatter diagrams plotted in this initial phase resemble that of Fig. 5, which characterize a ‘modon’. However, unlike in Fig. 4, this isolated structure cannot persist because Eq. (12) is not satisfied. The vortex pair is seen to drift westward, away from the forcing region, exciting Rossby waves in its lee which remove energy from the closed  $q$  contour region. (It is worthy of note that this tendency to drift westward is often observed in blocking episodes.) The initial rapid amplification local to the forcing gives way to a lower amplitude global response shown in Fig. 7(b) which more closely resembles the linear damped stationary Rossby wave of Fig. 6.

The two phases of this mixed response are conveniently summarized in Fig. 8 where the maximum amplitude of the eddy streamfunction is plotted against time. Curve A shows the pure modon response taken from Fig. 4, and curve B is the linear Rossby wave response of Fig. 6. Curve C (taken from Fig. 7) shows the mixed response with rapid growth in the first 15 days (closely following curve A) exhibiting modon characteristics (see Fig. 7(a)), followed by decay as stationary Rossby waves extract energy on a timescale of about 15 days.

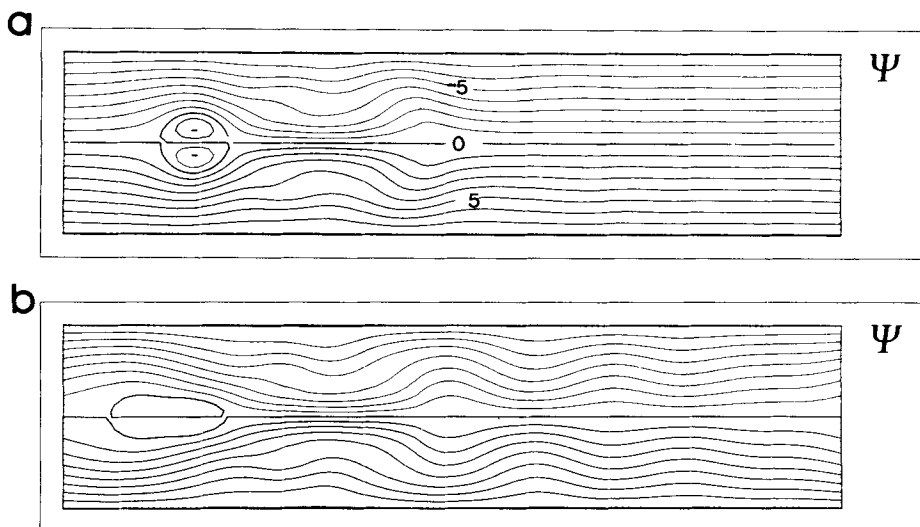


Figure 7. The flow response to the eddy forcing function in a fully nonlinear model Eq. (17) for mean flow parameters which allow stationary Rossby waves in the channel. The initial conditions, forcing and dissipation are as in Fig. 6. Despite being in a stationary Rossby wave regime the initial response after  $12\frac{1}{2}$  days (Fig. 7(a)) is local to the forcing and closely resembles a modon (compare with Fig. 4). By day 50, however, (Fig. 7(b)) the local nonlinear response has weakened giving way to an antisymmetric Rossby wave which more closely resembles the linear response shown in Fig. 6. Contours are plotted in units of  $\beta L_p^3$ .

Thus it can be seen that local coherent structures resembling blocks can persist for a significant time even in the presence of stationary Rossby waves if energy is removed from the closed  $q$  contour region at a rate which is slow compared with the recirculation time of trapped fluid parcels. This has important consequences for diagnostic studies of blocking, such as McWilliams (1980) which attempt to identify blocking with analytical modon theories. It may not be necessary for the mean flow to satisfy Eq. (12) which excludes stationary waves; if a localized forcing of the appropriate sign is present then nonlinear resonances can excite local free modes which can be identified with blocking, even though the mean flow does not satisfy Eq. (12).

#### 4. INTERACTION OF SYNOPTIC SYSTEMS WITH ISOLATED VORTEX PAIRS

In sections 2 and 3 a case has been presented for considering modons to be useful constructs in describing blocked configurations. It has been demonstrated that synoptic-scale eddies may provide (at least in a linearized small amplitude sense) a dipole vorticity forcing consistent with maintaining an isolated structure. However, although the isolated vortex pair may capture the essence of blocked configurations, it must be deficient in at least one respect for it implies that the trajectories of fluid parcels are coincident with the streamlines of Fig. 2, i.e. it assumes a steady state. However, time-dependence is an essential ingredient of the blocking mechanism allowing the trajectories of fluid parcels to cross time-mean streamlines and so admitting the possibility of ventilation and hence maintenance of the structures considered in sections 2 and 3. Thus, in this section the interaction of a field of large amplitude synoptic eddies with an isolated vortex pair is studied in a fully nonlinear model.

These integrations are inspired by the instructive sequences of high resolution IPV maps during a blocking episode recently prepared by Shutts (1986) and Hoskins *et al.* (1985) which clearly demonstrate the role of eddies in sustaining the blocked configur-



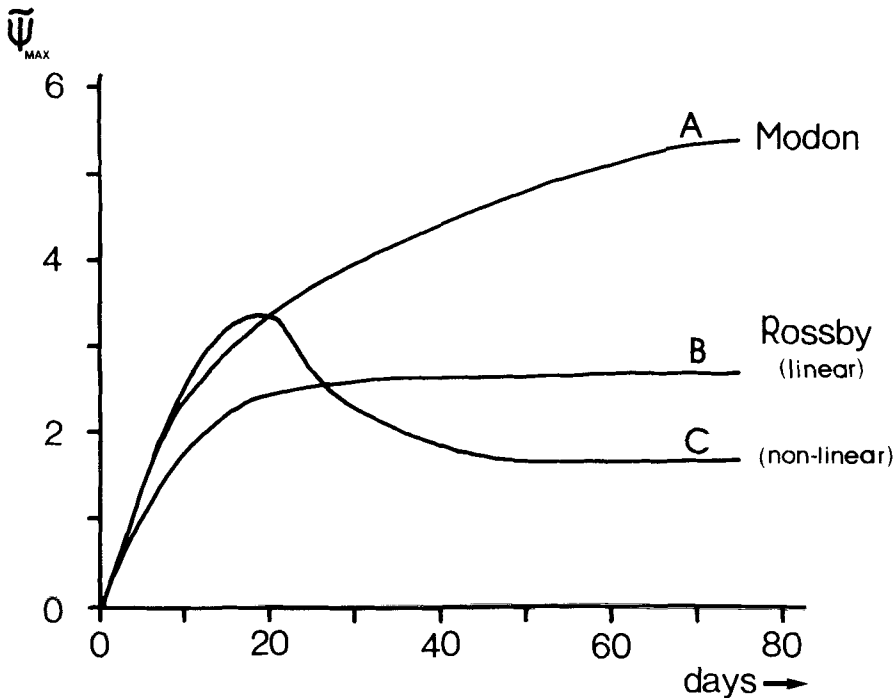


Figure 8. The maximum value of the eddy streamfunction plotted against time. Curve A is the pure modon response of Fig. 4. Curve B is the linear Rossby wave response of Fig. 6 and curve C, corresponding to Fig. 7, is the mixed modon/Rossby wave response. Initially the curve rises rapidly as in A, showing a resonant response local to the forcing. However, it peaks and begins to decay as stationary Rossby waves are excited in the lee, extracting energy on a timescale of  $\sim 15$  days.

ation: synoptic systems approaching from the west sweep low  $q$  air north into the anticyclone and then high  $q$  air south into the cyclone. The IPV map of 15 February shown in Fig. 1(b) is a particularly spectacular example. A narrow band of low potential vorticity air can be seen being swept northwards ( $30^\circ\text{W}$ ) on the eastern flank of the depression upstream of the vortex pair, filling the anticyclone. Further to the west a tongue of high  $q$  air sweeps southwards and will join to the high  $q$  air associated with the cyclone to the south.

There are many dynamical and thermodynamical processes at work in Fig. 1 which cannot be represented in an equivalent barotropic model. The synoptic systems interacting with the blocking high may be baroclinically active; energy release in moist processes particularly ahead of the cold front on the tongue of low  $q$  air extending northwards is undoubtedly important in the energetics of the quasi-stationary blocked configuration. However, it is of interest to study to what extent the morphology of the IPV maps can be understood in terms of the passive quasi-barotropic deformation of synoptic systems by the large-scale flow.

Thus the fully nonlinear equivalent barotropic model is initialized with a vortex pair in a zonal flow and finite amplitude eddy vortices of alternating sign are introduced upstream by means of a wavemaker. In order to study the interaction of the eddy field with the vortex pair all processes which are inimicable to the existence of the latter are excluded in the model. Thus in the numerical calculations the ambient  $\partial q_\infty/\partial y$  and zonal flow  $U$  are chosen so as to disallow stationary Rossby waves in the channel. The values chosen are close to those of the analytic solution Eq. (15) with  $U = 13.8 \text{ m s}^{-1}$  and  $q_\infty = 1.35\beta y$ . A stronger  $q$  gradient was chosen so that the modon has a small westward

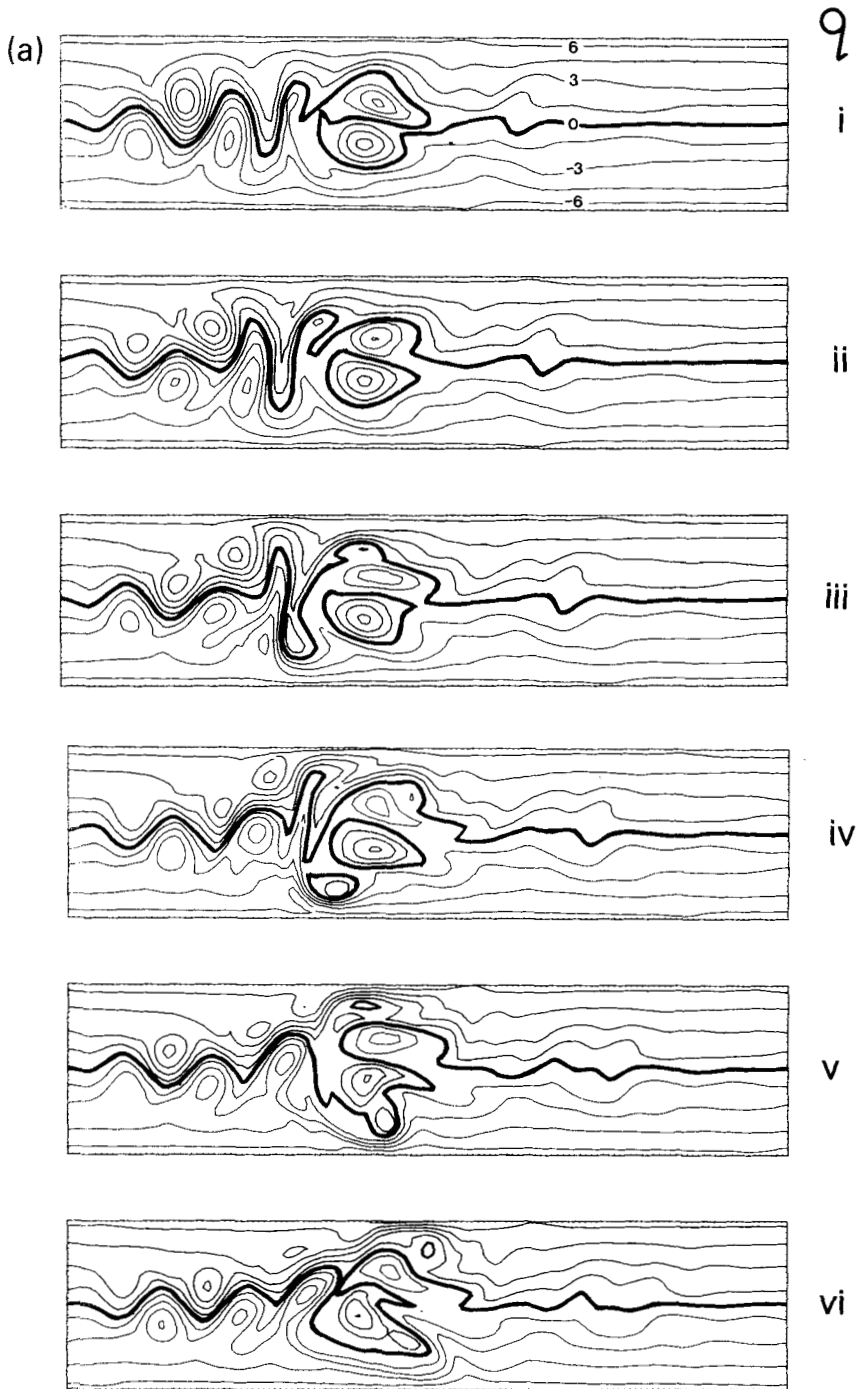


Figure 9. Time sequence of the instantaneous  $q$ , contour interval  $1.5\beta L_p$  (a); and  $\tilde{\psi}$ , contour interval  $1.0\beta L_p^3$  ( $\tilde{\psi} = \psi + Uy$ ) (b); fields at  $2\frac{1}{2}$  day intervals, showing the interaction between a train of eddies (generated by a wavemaker) and a modon placed in the zonal flow. Dissipation is through grid-point friction; there is no Ekman friction. The thick black lines in (a) are the zero contours and can be tentatively associated with the discontinuity in potential vorticity which marks the tropopause in Fig. 1(b). H and L label centres of high and low pressures. The channel was initialized with the modon solution of Eq. (15), with  $U = 13.8 \text{ ms}^{-1}$  and  $\partial q_\infty / \partial y = 1.35\beta$  in the far field.

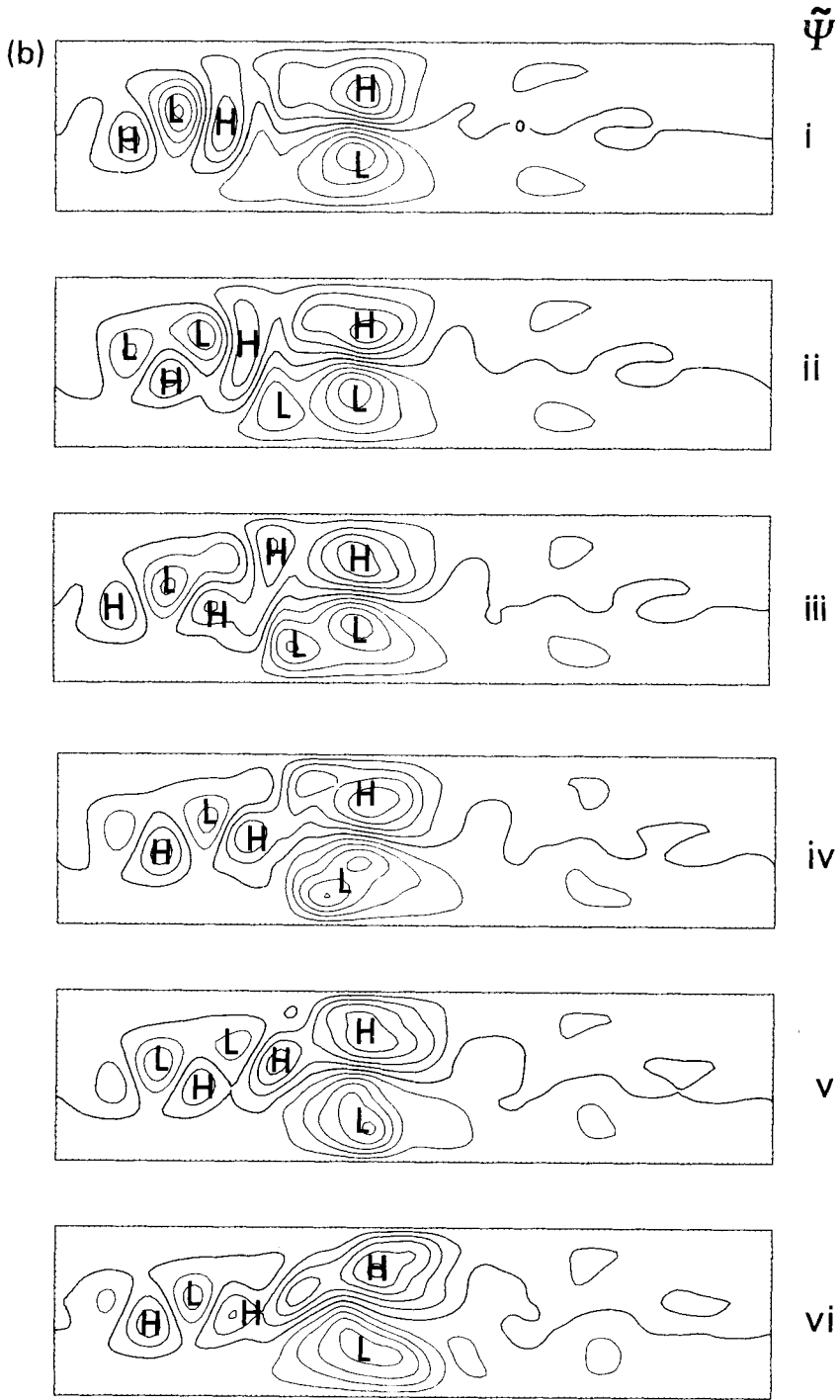


Figure 9—continued

drift velocity giving stronger eddy/mean flow interactions. A grid-scale diffusion  $\nu \nabla^6 \psi$  removes the enstrophy at the grid-scale allowing irreversible breaking of the  $q$  contours. The e-folding time associated with the scale-selective diffusion is 250 days on the scale of the modon: no bottom friction is included.

A sequence of model synoptic maps at  $2\frac{1}{2}$  days intervals is shown in Fig. 9(a) (potential vorticity) and Fig. 9(b) (eddy streamfunction) allowing the interaction of the eddies with the vortex pair to be studied.

In order to draw comparison with the IPV maps the zero contour in Fig. 9(a) can be tentatively associated with the sharp gradient of IPV in Fig. 1(b) marking the transition at the tropopause between high  $q$  stratospheric air to the north and low  $q$  tropospheric air to the south. With this interpretation then, the thick black line in Fig. 9(a) is the tropopause undulating north and south under the action of the wavemaker.

As they leave the wavemaker region the cyclones (marked L in Fig. 9(b)) are seen to align along a latitude somewhat to the north of the mid-channel and the anticyclones (marked H) somewhat to the south (an effect which is absent in the linear model of section 3). Rossby (1948) interprets this in terms of the tendency of vortices to migrate meridionally to their reference latitudes. The jet is accelerated at mid-channel by this process as the orientation of the trough lines, sloping NW to the north and SW to the south, is in a sense to feed westerly momentum into the jet (see Fig. 9(a)).

The eddy vortices are intense enough to cause troughs and ridges to cut off from the main current occasionally forming cyclonic vortices to the south and anticyclonic vortices to the north. This process is particularly evident in the  $q$  fields in which blobs of  $q$  cut off in a manner which is reminiscent of Gulf Stream rings. This meridional exchange of potential vorticity is dramatically enhanced just upstream of the vortex pair where the east-west scale of the approaching vortices undergoes a compression, meridional velocities increase and fluid parcels thus experience large north-south excursions. Ahead of an approaching cyclonic vortex (L) air parcels are swept northwards from southerly latitudes (Figs. 9(a), (i), (ii) and (iii)) carrying with them their low  $q$  values. To the rear of this low pressure system a narrow tongue of high  $q$  air can be seen being advected south (Fig. 9(a) (iii)) by strong northerly winds. This process can be seen clearly in the  $q$  maps which allow the trajectories of fluid parcels to be inferred. In contrast, the height field, Fig. 9(b), which might be thought of as the corresponding surface pressure map, is not a materially conserved quantity and gives a blurred image of the same process.

The presence of a small scale-selective lateral friction ensures that these meridionally orientated tongues of  $q$  do not continue to extend and narrow indefinitely, but allows them to break; the deformation of the  $q$  contours is irreversible. This 'wave breaking' is well illustrated by following the time development of the zero contour in Fig. 9(a). In the region of the wavemaker the zero contour (tropopause) undulates north and south reversibly with no appreciable eddy/mean flow interaction. Upstream of the  $q$  anomaly, however, the zero contour undergoes marked contortions as the waves propagating along the sharp potential vorticity gradient at the tropopause 'break' on encountering the split jet. This folding over of the  $q$  contours is indicative of irreversible processes (visible evidence of the enstrophy cascade) and meridional transfer of potential vorticity. The meridional potential vorticity gradient is overturned with low  $q$  air transferred north, high  $q$  air south implying strong southward eddy potential vorticity fluxes. This acts as a westward force in the zonal momentum equation decelerating the flow and splitting the jet.

This sequence of generation of wave activity by baroclinic processes (represented by the wavemaker), propagation and deposition as the waves break on encountering the split jet can be elegantly presented in terms of the 'E-vector' diagnostics developed by

Hoskins *et al.* (1983). The vector  $\mathbf{E} = (\overline{v'^2 - u'^2}, -\overline{u'v'})$  has useful properties since it nearly points in the direction of the group velocity relative to the mean flow for Rossby waves. Furthermore, its divergence is a measure of the time-mean forcing of westerly momentum exerted by the eddy field on the mean flow.

The  $\mathbf{E}$  vector derived from eddy statistics computed over a 20-day sequence of model fields is shown in Fig. 10. The storm track is clearly evident with the  $\mathbf{E}$  vectors pointing eastwards,  $\overline{v'^2} > \overline{u'^2} > |\overline{u'v'}|$ , typical of the eddy statistics appropriate to the high-pass filtered synoptic-scale systems which are elongated in the meridional direction. In the wavemaker region eddy activity is generated and there is a divergence of the  $\mathbf{E}$  vector. Mid-way along the track the vectors show a tendency to fan out as the wave flux begins to propagate meridionally and trough lines become bowed. In these regions of  $\mathbf{E}$ -vector divergence the mean flow jet is accelerated eastwards. However, in the region of the split jet there is strong  $\mathbf{E}$ -vector convergence implying a deceleration of the westerlies. The  $\mathbf{E}$  vectors tend to divide following the two branches of the split jet. However, they also show a tendency to point toward the region of weak zonal flow, a feature of  $\mathbf{E}$  vectors during a blocking episode noted by Hoskins *et al.* This is consistent with the changing orientation of the synoptic-scale systems as they move in the split jet, becoming meridionally extended and overturned. In this region of strong deformation there is a sink of wave activity (eddy enstrophy) with  $\mathbf{E}$ -vector convergence. This is evident from the sequence of  $q$  maps in Fig. 9(a): once the deformation of the  $q$  contours becomes irreversible, then the existence of an enstrophy sink is inevitable and all that goes with it—down-gradient  $q$  fluxes and systematic effects of eddies on mean flow. Thus we see that the interaction between the train of travelling vortices and the stationary vortex pair is in a sense to sustain the vortex pair which then grows in intensity.

The integration shown in Fig. 9 was continued for two months; the dipole continued to intensify throughout as it entrained vorticity of appropriate sign, expanding in scale and eventually moving off downstream. That this can occur in our two-dimensional model suggests that much of the structure to be seen in the IPV sequence can be understood largely in terms of the passive deformation of synoptic-scale vortices by the larger-scale flow: thus baroclinic processes may not be playing a dominant role here at the end of the storm track.

Many integrations with various initial conditions and wavemaker intensities were carried out in addition to that presented in Fig. 9. Often the vortex pair would be overturned on interaction with a particularly intense eddy, with the  $q$  anomaly being reabsorbed into the appropriate reservoir, high  $q$  to the north and low  $q$  to the south.

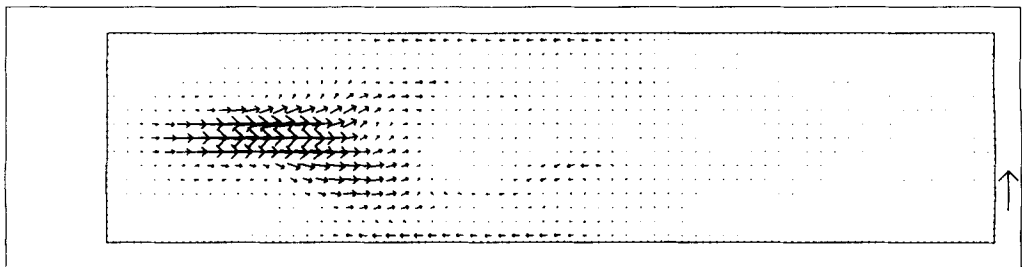


Figure 10. The  $\mathbf{E}$  vector,  $= (\overline{v'^2 - u'^2}, -\overline{u'v'})$ , in units of  $250 \text{ m}^2 \text{ s}^{-2}$ , (indicated by the arrow in the margin, bottom right) calculated from a 20-day model sequence including the period shown in Fig. 9. The  $\mathbf{E}$  vectors point eastward indicating downstream propagation of energy relative to the mean flow. In the storm-track/wavemaker region where there is genesis of eddy energy the  $\mathbf{E}$  vectors diverge. In the blocking region at the end of the storm track where eddy energy is transferred up-scale into the straining field, the  $\mathbf{E}$  vectors converge.

However, occasionally, subsequent to the break-up of the modon configuration, it was replaced by another blocking dipole which formed spontaneously after meridional vorticity transfer by the transient systems.

Finally we contrast the flow response described in this section with that of a flow in which stationary Rossby waves can be excited, such as in the model of Shutts (1983). If in the fully nonlinear model a wavemaker is used to introduce eddy vortices into a zonal flow which can support stationary Rossby waves, the flow spontaneously splits downstream of the wavemaker and an antisymmetric stationary Rossby wave is excited. The splitting of the jet is directly associated with the presence of the wavemaker and so, by implication, with baroclinic processes. Although this is a perfectly plausible mechanism by which one can sustain a split jet (and is the one advocated by Shutts) it is not at work in the sequence shown in Fig. 9.

## 5. DISCUSSION

In this study attention has been focused on two important aspects of atmospheric blocking, namely its localized nature and its maintenance through interaction with travelling synoptic-scale systems. It has been argued that the close coincidence of  $\psi$  and  $q$  contours suggests that the atmosphere is in an almost free configuration: of particular relevance to the dynamics of blocking is the observation that the  $q$  contours at upper levels are closed off suggesting that local nonlinear free modes might be a useful starting point from which to consider the dynamics of blocking. Accordingly the equivalent barotropic modon of McWilliams (1980) has been reconsidered as a prototype of atmospheric blocking since it bears such a striking resemblance to Atlantic blocking configurations.

It has been demonstrated that the anomalous transfer of potential vorticity induced by the straining of eddies in a diffuent flow is in the sense to sustain the modon. This result was anticipated by Shutts (1983) and supporting evidence from observational data discussed in Illari and Marshall (1983) and Illari (1984).

Perhaps the most striking aspect of our study, however, is the ease and vigour with which nonlinear free modes can be excited by a localized forcing of the appropriate form. Indeed so rapid is the growth, even in response to moderate forcing, that nonlinear structures resembling vortex pairs can exist for significant periods even in the presence of stationary Rossby waves. Although the response is almost free, it is the presence of weak forcing and dissipation which picks out a unique solution.

Our experiments have some similarity to those carried out by PM who looked for localized multiple equilibria in a barotropic model. The modon could be considered a high amplitude state of the atmosphere, the stationary Rossby wave a low amplitude state. Our experiments indicate that the high amplitude state can exist on blocking timescales depending on whether it is being resonantly forced and on how efficiently the growing isolated structure loses energy by exciting Rossby waves in its lee. Further modelling work is required to investigate more closely these competing effects, but perhaps the most pressing need is for a reassessment of the observational evidence for localized modon-like structures during blocking events. It has been demonstrated that non-compliance with the analytical existence condition Eq. (12) does not rule out the presence of modons on blocking timescales although it may be important in determining the lifetime and stability of blocking structures. The study of McWilliams (1980) was inconclusive as to whether Eq. (12) is satisfied by the zonal, time-mean winds; he suggested that the atmosphere is near to the existence threshold for equivalent modons,

supporting the speculation that the comparative rareness of blocking is due to the infrequency with which Eq. (12) is satisfied.

Nonlinear resonance studies, such as the one described here, call for diagnostic studies which are directed towards identifying the signature of nonlinear localized free modes during blocking episodes. Instead of testing for the condition Eq. (12), one possible way to identify local free modes in atmospheric data is to use scatter diagrams similar to the one presented in Fig. 5 for our model data. Fortunately high quality, high resolution IPV maps are now available from ECMWF analysed fields, which are ideally suited for this purpose. Work is underway to interpret these data in terms of nonlinear free mode structures, the prototype of which is the equivalent barotropic modon studied here.

Should it turn out that the equivalent modon is, in detail, an inappropriate description of blocking, then other local structures such as the spatially isolated weakly nonlinear Rossby waves, studied by Malguzzi and Malanotte-Rizzoli (1984), could equally well be adopted as a zero-order field. It could then be anticipated that the interaction of these weakly nonlinear structures with travelling synoptic-scale systems, and their resonant forcing by them, would be much as described here. It should be noted though, that the observations suggest, Fig. 1, that blocking at upper levels is a strongly rather than a weakly nonlinear phenomenon.

The present modelling study could be extended in several ways. An investigation into the stability of isolated vortex pairs in a barotropic model with full spherical geometry would be of interest: meridional propagation of energy could then proceed unimpeded by the presence of channel walls and so the maintenance of localized structures on the sphere may be more problematical. Further studies using baroclinic models are needed in which the flow instability is explicit rather than represented by a wavemaker. However, we should like to conclude by suggesting that perhaps generally more attention should be given to the relevance of nonlinear free modes and nonlinear resonance to the atmosphere, both locally and on global scales. Here attention has been focused on one particularly simple nonlinear free mode existing in a uniform zonal flow, but presumably other solitary waves and modons existing in more general non-uniform mean flows can be constructed or resonantly excited. The observed close coincidence of the  $\psi$  and  $q$  contours in the upper troposphere indicates that the atmosphere may adjust through a succession of nonlinear free mode states and suggests that we ought to have an intense interest in solutions of the form  $q = q(\psi)$  and their resonant forcing.

#### ACKNOWLEDGMENTS

We should like to thank Drs Hide, Read, Shutts and White of the Meteorological Office for their continued interest and support during this study.

#### REFERENCES

- |   |      |  |
|---|------|--|
| Arakawa, A.                                 | 1966 | Computational design for long-term numerical integration of the equations of fluid motion: Two-dimensional incompressible flow: Part 1. <i>J. Comput. Phys.</i> , <b>1</b> , 119–143 |
| Baines, P. G.                               | 1983 | A survey of blocking mechanisms, with application to the Australian region. <i>Aust. Meteorol. Mag.</i> , <b>31</b> , 27–36  |
| Batchelor, G. K.                            | 1956 | Steady laminar flow with closed streamlines at large Reynolds numbers. <i>J. Fluid Mech.</i> , <b>1</b> , 177–190  |
| Berggren, R., Bolin, B. and<br>Rosby, C. G. | 1949 | An aerological study of zonal motion, its perturbation and breakdown. <i>Tellus</i> , <b>1</b> , 14–37   |

- Dole, R. M. and Gordon, N. D. 1983 Persistent anomalies of the extratropical Northern Hemisphere wintertime circulation: Geographical distribution and regional persistence characteristics. *Mon. Weather Rev.*, **11**, 1567–1586
- Flierl, G. R., Larichev, V. D., McWilliams, J. C. and Reznik, G. M. 1980 The dynamics of baroclinic and barotropic solitary eddies. *Dyn. Atmos. Ocean*, **5**, 1–41
- Green, J. S. A. 1977 The weather during July 1976: Some dynamical considerations of the drought. *Weather*, **32**, 120–128
- Hoskins, B. J., James, I. and White, G. 1983 The shape, propagation and mean-flow interaction of large-scale weather systems. *J. Atmos. Sci.*, **40**, 1595–1612
- Hoskins, B. J., McIntyre, M. E. and Robertson, A. 1985 On the use and significance of isentropic potential vorticity maps. *Q. J. R. Meteorol. Soc.*, **111**, 877–946
- Illari, L. 1984 A diagnostic study of the potential vorticity in a warm blocking anticyclone. *J. Atmos. Sci.*, **41**, 3518–3526
- Illari, L. and Marshall, J. C. 1983 On the interpretation of maps of eddy fluxes. *ibid.*, **40**, 2232–2242
- McIntyre, M. E. and Palmer, T. N. 1983 Breaking planetary waves in the stratosphere. *Nature*, **305**, 593–600
- McWilliams, J. C. 1980 An application of equivalent modons to atmospheric blocking. *Dyn. Atmos. Ocean*, **5**, 43–66
- Malguzzi, P. and Malanotte-Rizzoli, P. 1984 Non-linear stationary Rossby waves on non-uniform zonal winds and atmospheric blocking. Part I: The analytical theory. *J. Atmos. Sci.*, **41**, 2620–2628
- Marshall, J. C. and Nurser, G. 1986 Steady, free circulation in a stratified quasi-geostrophic ocean. *J. Phys. Oceanogr.*, **16**, 1799–1813
- Niiler, P. P. 1966 On the theory of wind-driven ocean circulation. *Deep-Sea Res.*, **13**, 597–606
- Pierrehumbert, R. T. and Malguzzi, P. PM 1984 Forced coherent structures and local multiple equilibria in a barotropic atmosphere. *J. Atmos. Sci.*, **41**, 246–257
- Rhines, P. B. and Young, W. R. 1982 Homogenization of potential vorticity in planetary gyres. *J. Fluid Mech.*, **122**, 347–369
- Rossby, C. G. 1948 On displacements and intensity changes of atmospheric vortices. *J. Mar. Res.*, **7**, 175–187
- Shutts, G. J. 1983 The propagation of eddies in diffluent jetstreams: Eddy vorticity forcing of 'blocking' flow fields. *Q. J. R. Meteorol. Soc.*, **109**, 737–761
- 1986 A case study of eddy forcing during an Atlantic blocking episode. *Adv. Geophys.*, **29**, 135–161